

## Supplementary Online Material

Marco Laurati<sup>a,b</sup>, Tatjana Sentjabrskaja<sup>b</sup>, José Ruiz-Franco<sup>c</sup>, Stefan U. Egelhaaf<sup>b</sup>, and Emanuela Zaccarelli<sup>c,d</sup>  
<sup>a</sup> *División de Ciencias e Ingeniería, Universidad de Guanajuato, Loma del Bosque 103, 37150 León, Mexico*  
<sup>b</sup> *Heinrich Heine University, Universitätsstraße 1, 40225 Düsseldorf, Germany*  
<sup>c</sup> *Dipartimento di Fisica, Università di Roma “La Sapienza”, Piazzale A. Moro 2, 00185 Roma, Italy and*  
<sup>d</sup> *CNR-ISC, Università di Roma “La Sapienza”, Piazzale A. Moro 2, 00185 Roma, Italy*

### Additional Structural Data

Figs. S1 and S2 show simulation results for the partial static structure factors of large and small particles,  $S_{LL}(q)$  and  $S_{SS}(q)$ , respectively, for different volume fractions  $\phi$ , size ratios  $\delta$  and compositions  $x_s$ . These data complement the data in Fig.1 of the main manuscript for  $\phi = 0.62$ . As it can be seen, changes in volume fraction do not affect the qualitative features of the structure factors presented in Fig.1 of the main manuscript, they mainly affect the height of the peaks.

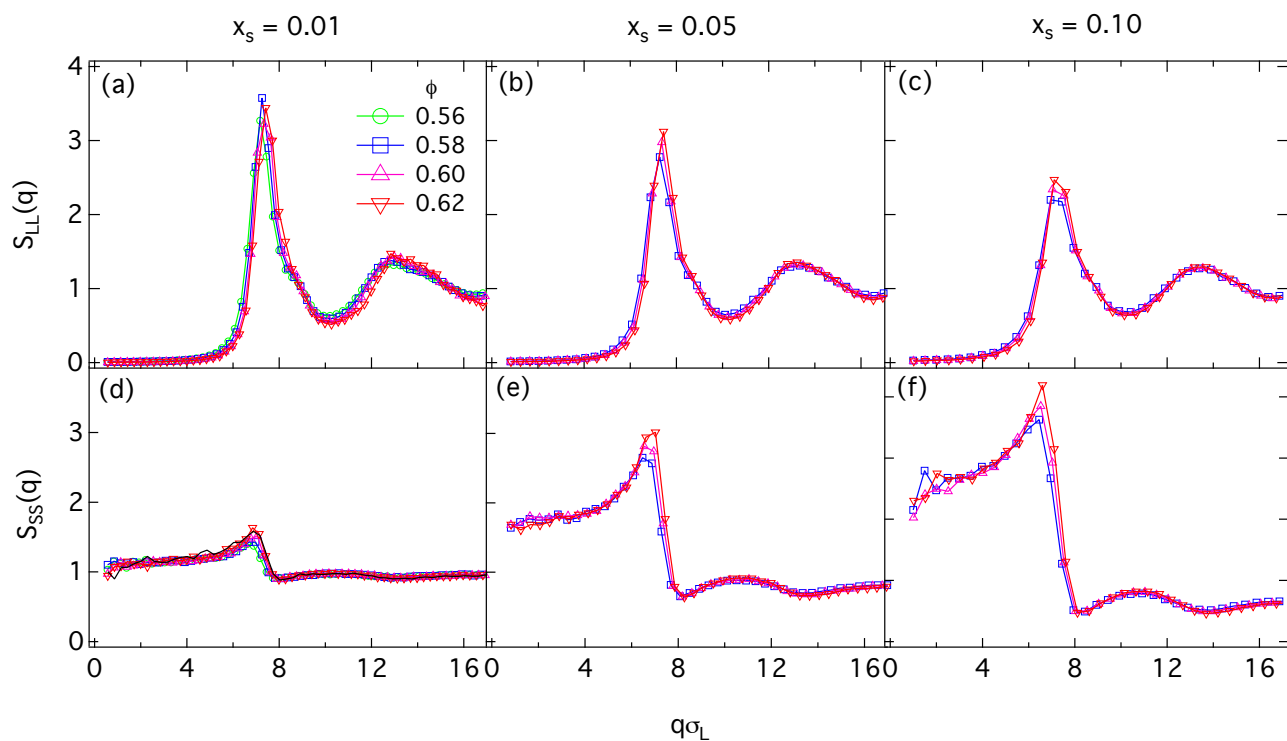


FIG. S1: Static structure factors of (a,b,c) the large particles,  $S_{LL}(q)$ , and (d,e,f) of the small particles,  $S_{SS}(q)$ , from simulations for size ratio  $\delta = 0.20$ , different volume fractions  $\phi$  and different fractions of small particles  $x_s$ .

In addition, Fig. S3 completes the data reported in Fig.1 of the manuscript with the partial static structure factors of large and small particles for  $\delta = 0.5$ . While  $S_{LL}(q)$  has a very similar behavior to the other size ratios reported in the manuscript, showing only a decrease of the peaks with increasing  $x_s$ ,  $S_{SS}(q)$  displays a behavior that is distinct from the other two size ratios: the usual dependence for  $x_s = 0.01$  is followed by the occurrence of a dip (rather than a peak) for  $\delta = 0.05$  and  $0.10$  which corresponds to the first peak of  $S_{LL}(q)$  of the large particles. This indicates the strong coupling between large and small particles at this size ratio.

### Additional Dynamical Data

Figs. S4 and S5 present simulation results for the collective intermediate scattering functions  $f(q, \Delta t)$  of large and small particles obtained for different volume fractions  $\phi$ , compositions  $x_s$  and size ratios  $\delta$ . These data complement

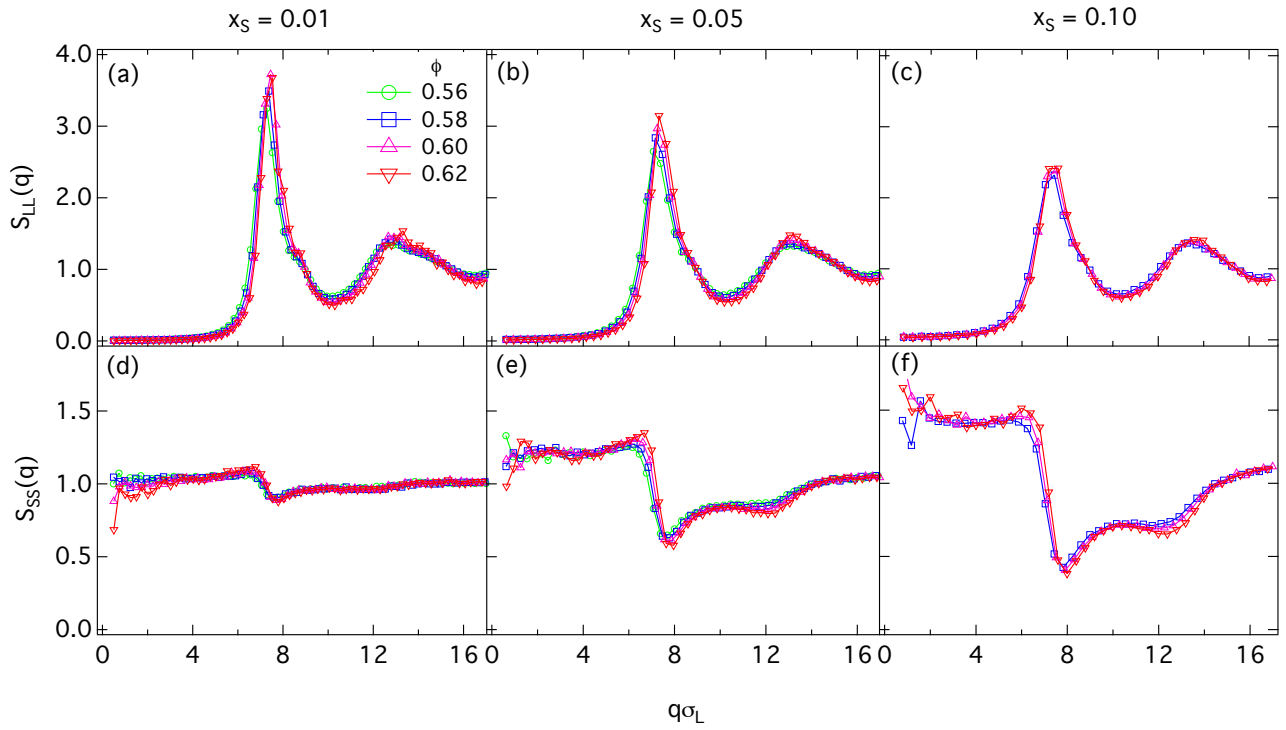


FIG. S2: Static structure factors of (a,b,c) the large particles,  $S_{LL}(q)$ , and (d,e,f) of the small particles,  $S_{SS}(q)$ , from simulations for size ratio  $\delta = 0.35$ , different volume fractions  $\phi$  and different fractions of small particles  $x_s$ .

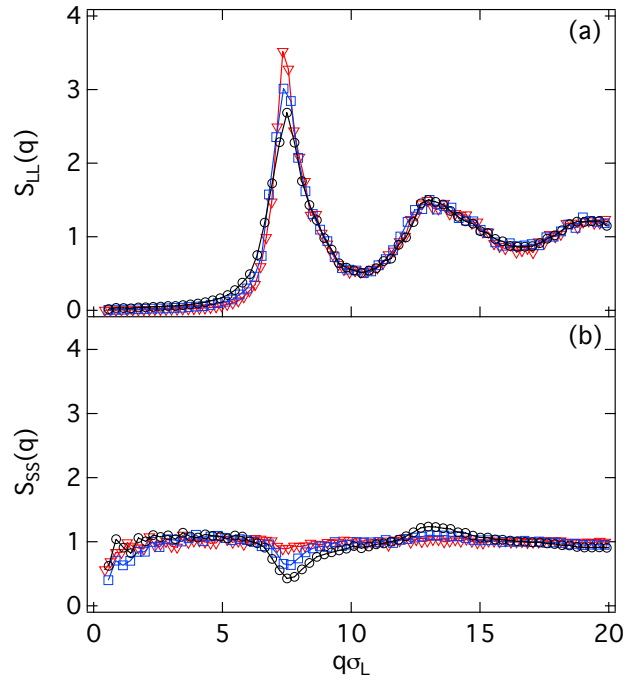


FIG. S3: Static structure factors of (a) the large particles,  $S_{LL}(q)$ , and (b) small particles,  $S_{SS}(q)$  from simulations for size ratio  $\delta = 0.5$ , volume fraction  $\phi = 0.62$  and different fractions of small particles  $x_s = 0.01$  (triangles),  $0.05$  (squares) and  $0.10$  (circles).

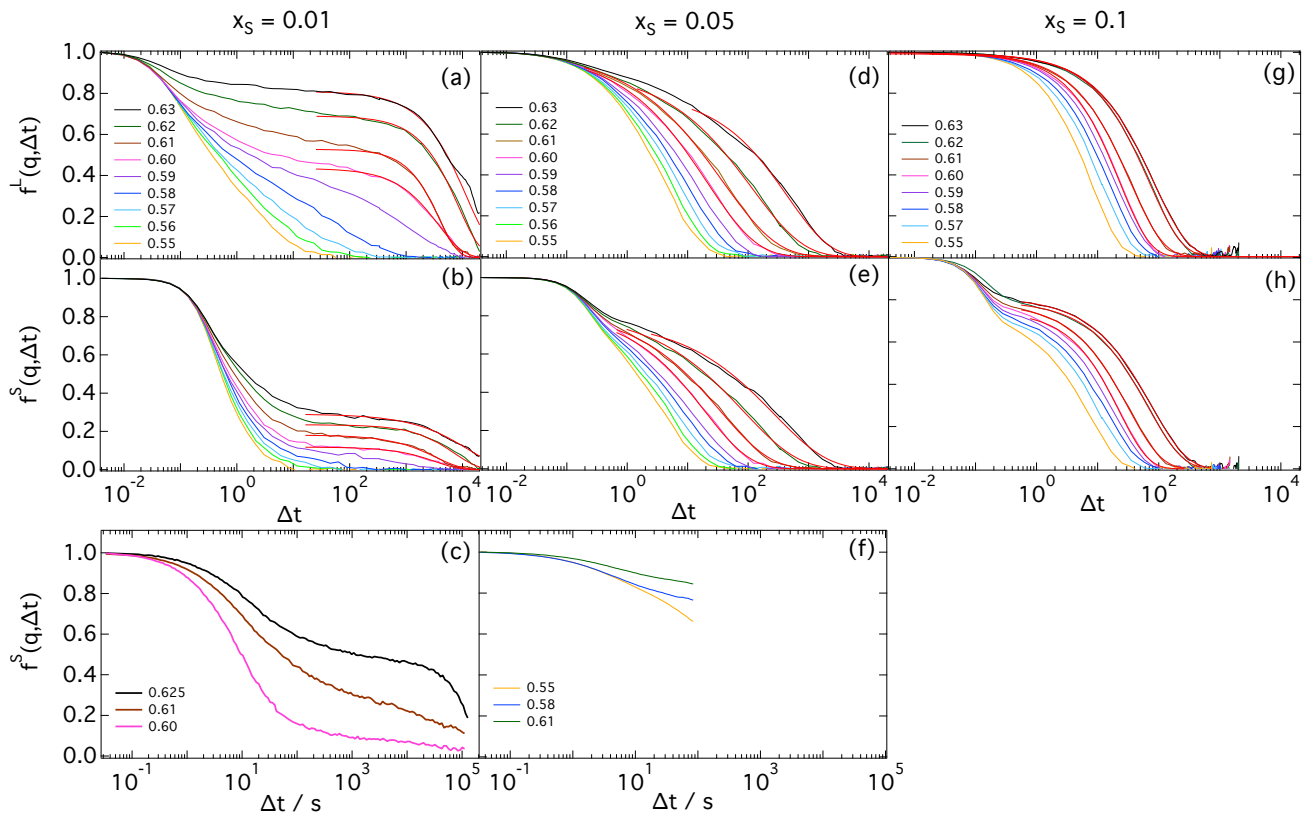


FIG. S4: Intermediate scattering functions  $f(q, \Delta t)$  for  $\delta = 0.2$ ,  $q\sigma_l = 3.5$ , different volume fractions  $\phi$  and different values of  $x_s$ . Top graphs (a,d,g) show results of simulations for the large particles, mid graphs (b,e,h) for the small particles. Red lines in (a,b,d,e,g,h) represent fits of the long time relaxation of  $f(q, \Delta t)$  according to Eq.6 of the main manuscript. Bottom graphs (c,f) show corresponding experimental results for the small particles for  $\delta = 0.18$ .

those of Fig.2 of the main manuscript for  $\phi = 0.62$ . As it can be seen, the reduction in total volume fraction  $\phi$  results in a progressive acceleration of the decay of  $f(q, \Delta t)$ , associated with the dilution of the system. It is interesting to note in Fig.S5 that for  $\delta = 0.35$  the anomalous logarithmic relaxation for the small particles is observed over the whole time window only for the largest total volume fraction,  $\phi = 0.63$ , while for the smaller total volume fractions it reduces to a shorter time interval.

Fig. S6 shows the collective intermediate scattering functions  $f(q, \Delta t)$  obtained for  $\phi = 0.62$ ,  $q\sigma_l = 3.5$ , different compositions  $x_s$  and size ratios  $\delta$ . These data complement those presented in Fig.4 of the main manuscript. It can be seen that with decreasing size disparity (increasing  $\delta$ ) the dynamics of the small and large particles become increasingly comparable at short and long times, indicating the formation of mixed cages.

### Fit parameters

Fit parameters obtained by fitting a stretched exponential function according to Eq.6 of the main article to  $f(q, \Delta t)$  of the large and small particles from simulations (Figs. S7 and S8) and experiments (Fig. S9). For the small particles and  $\delta = 0.35$  and  $x_s = 0.01$  conditions, Eq.7 of the main manuscript was used and, in agreement with previous work[1]  $\tau_{\log} = 5$  was fixed. These data complement those reported in Figs. 5 and 6 of the main article. The coupling of the dynamics of the two species, already discussed in the main article for  $\phi = 0.62$ , is present also for other total volume fractions  $\phi$ , as can be seen by comparing the long-time relaxation times of the small and large particles,  $\tau_{LO}^S$  and  $\tau_{LO}^L$ , respectively, as well as the plateau heights  $f_c^S$  and  $f_c^L$ , respectively. The small values of the stretching exponents found for essentially all samples evidence the broad distribution of relaxation times of the small particles.

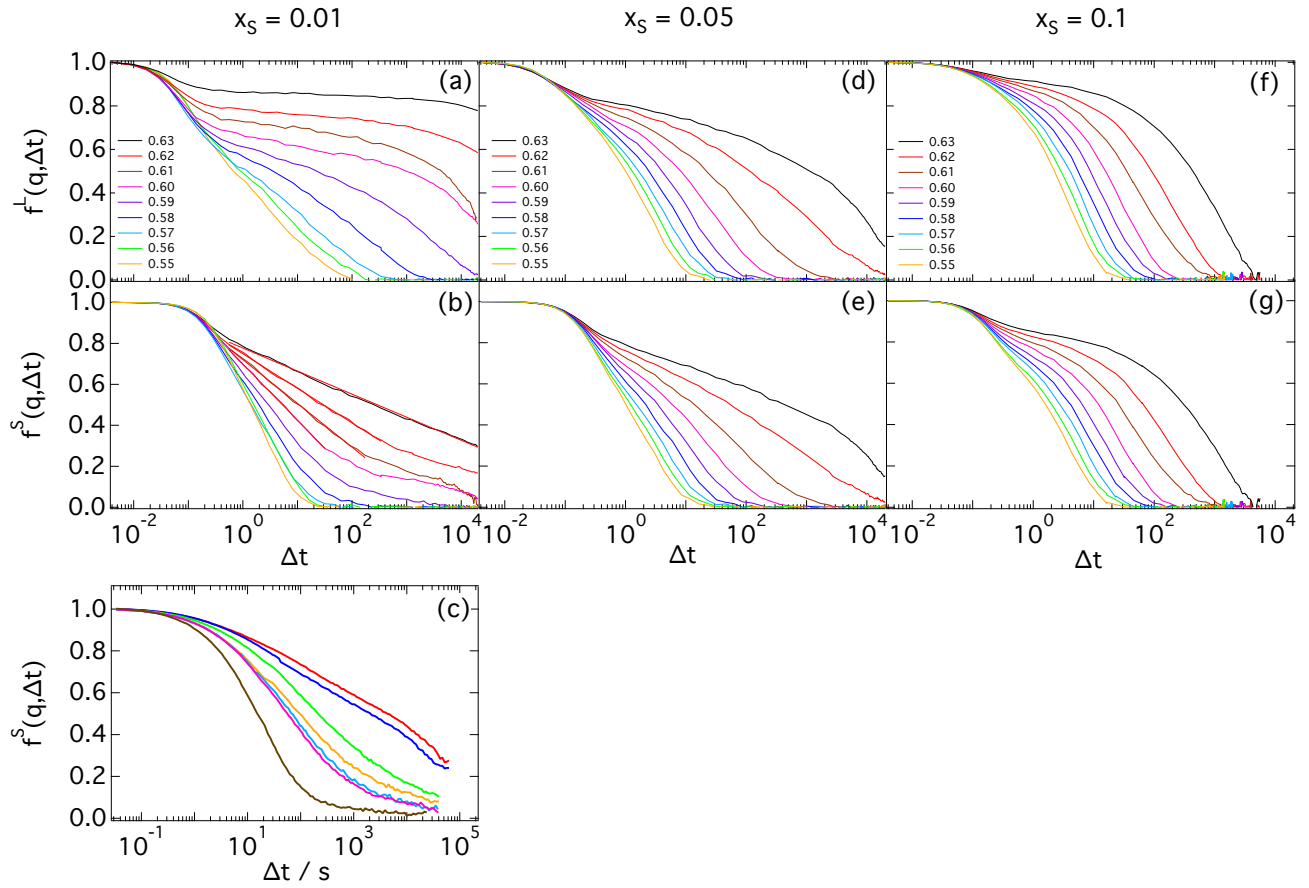


FIG. S5: Intermediate scattering functions  $f(q, \Delta t)$  for  $\delta = 0.35$ ,  $q\sigma_l = 3.5$ , different volume fractions  $\phi$  and different values of  $x_s$ . Top graphs (a,d,g) show results of simulations for the large particles, mid graphs (b,e,h) for the small particles. Red lines in (b) represent fits of the logarithmic relaxation of  $f(q, \Delta t)$  according to Eq.7 of the main manuscript. Bottom graph (c) shows corresponding experimental results for the small particles for  $\delta = 0.28$ .

---

[1] C. Mayer, F. Sciortino, C. N. Likos, P. Tartaglia, H. Löwen and E. Zaccarelli, *Macromolecules*, 2009, **42**, 423–434

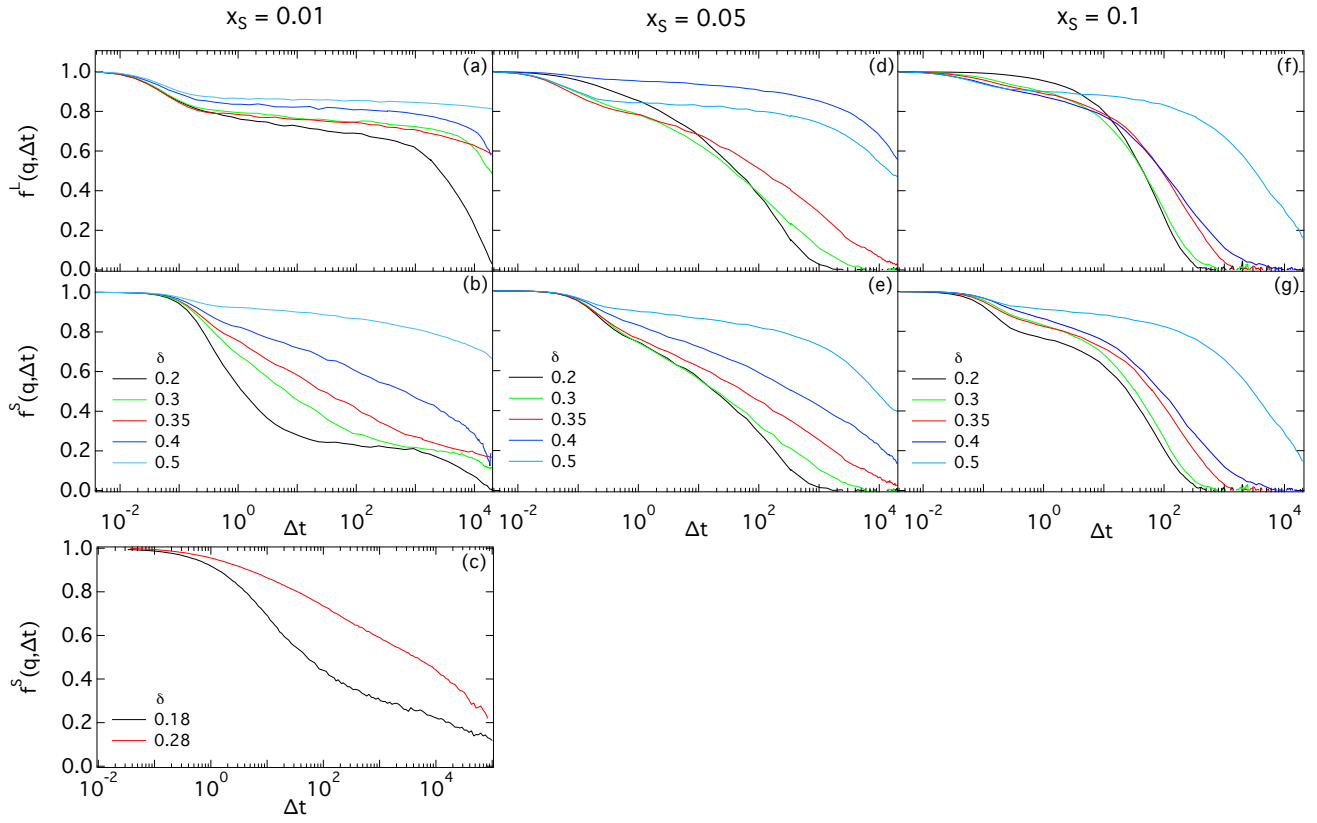


FIG. S6: Intermediate scattering functions  $f(q, \Delta t)$  for different  $\delta$ ,  $q\sigma_l = 3.5$  and different values of  $x_s$ : Top graphs (a,d,f) show results of simulations for the large spheres,  $\phi = 0.62$ , mid graphs (b,e,g) for the small particles,  $\phi = 0.62$ . Bottom graph (c) shows corresponding experimental results for small particles and  $\phi = 0.61$ .

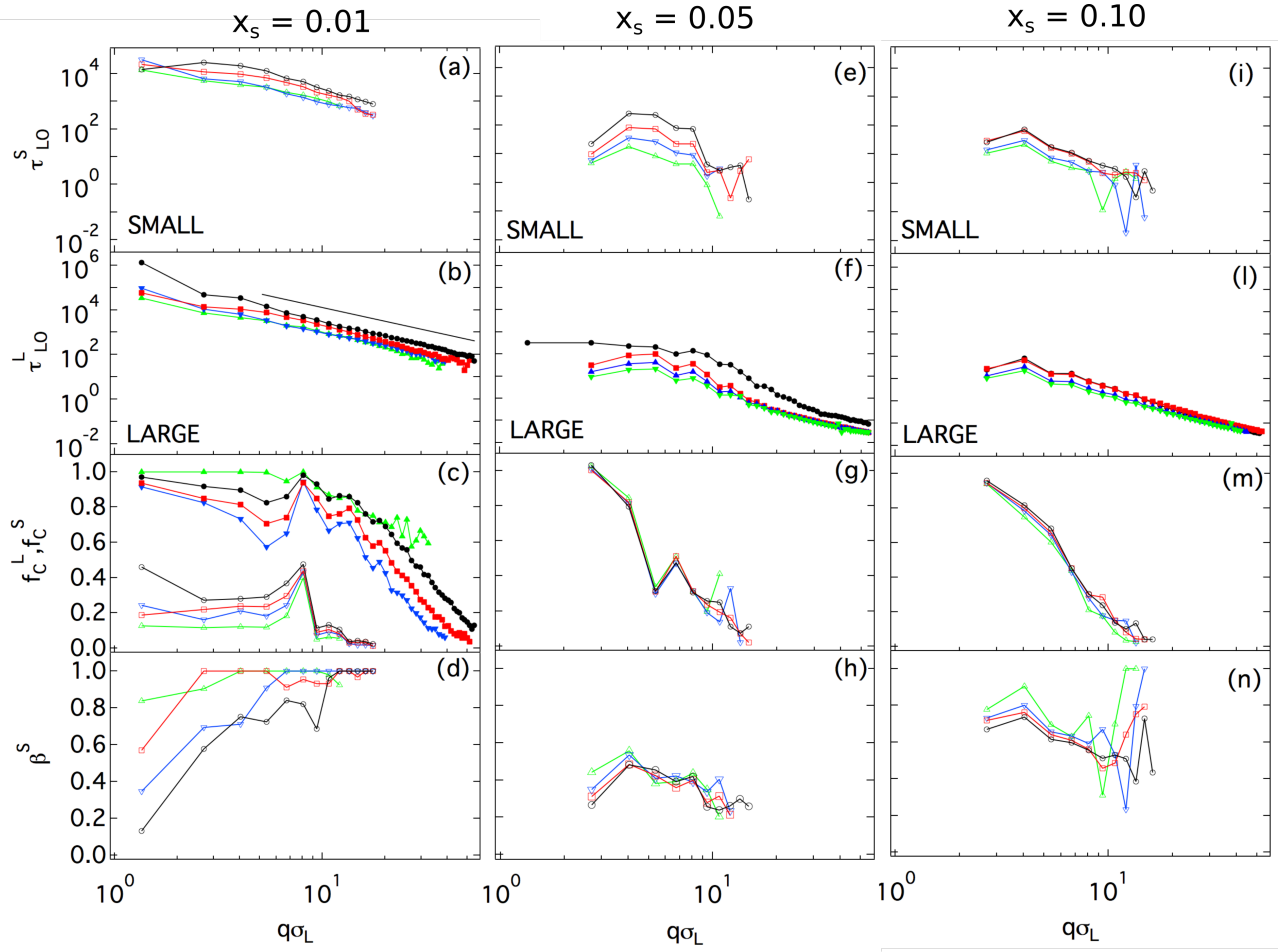


FIG. S7: Parameters obtained by fitting Eq. 6 of the main manuscript to  $f(q, \Delta t)$  from simulations for  $\delta = 0.2$ ,  $\phi = 0.60$  ( $\triangle$ ), 0.61 ( $\nabla$ ), 0.62 ( $\square$ ) and 0.63 ( $\circ$ ) and  $x_s = 0.01$  (left column), 0.05 (mid column) and 0.1 (right column), as a function of  $q\sigma_L$ . (a), (e), (i): Long-time relaxation times for the small particles,  $\tau_{LO}^S$  (open symbols). (b), (f), (l): Long-time relaxation times for the large particles,  $\tau_{LO}^L$  (full symbols). (c), (g), (m): Plateau height for the large,  $f_c^L$  (full symbols, when present), and small,  $f_c^S$  (open symbols), particles. (d), (h), (n): Stretching exponent  $\beta^S$  obtained from the fits to the long-time relaxation of the small particles.

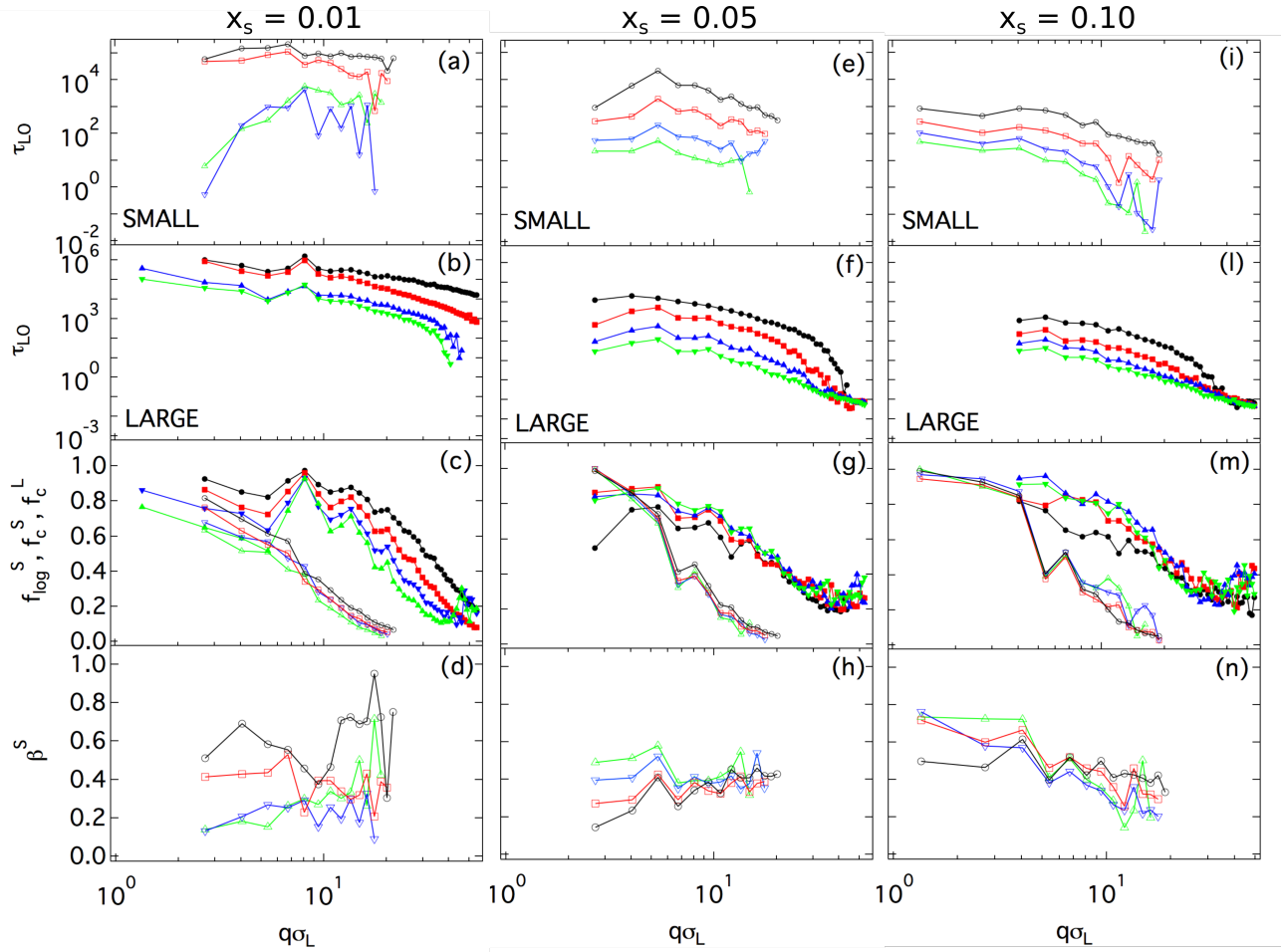


FIG. S8: Parameters obtained by fitting Eq. 6 of the main manuscript to  $f(q, \Delta t)$  from simulations for  $\delta = 0.35$ ,  $\phi = 0.62$  and  $x_s = 0.01$  ( $\square$ ),  $0.05$  ( $\circ$ ),  $0.10$  ( $\triangle$ ), as a function of  $q\sigma_L$ . (a), (e), (i): Long-time relaxation times for the small particles,  $\tau_{LO}^S$  (open symbols). (b), (f), (l): Long-time relaxation times for the large particles,  $\tau_{LO}^L$  (full symbols). (c), (g), (m): Plateau height for the large,  $f_c^L$  (full symbols, when present), and small,  $f_c^S$  (open symbols), particles. For  $x_s = 0.01$  we report the logarithmic non-ergodicity parameter  $f_{log}^S$  as defined in Eq.7 of the main manuscript. (d), (h), (n): Stretching exponent  $\beta^S$  obtained from the fits to the long-time relaxation of the small particles.

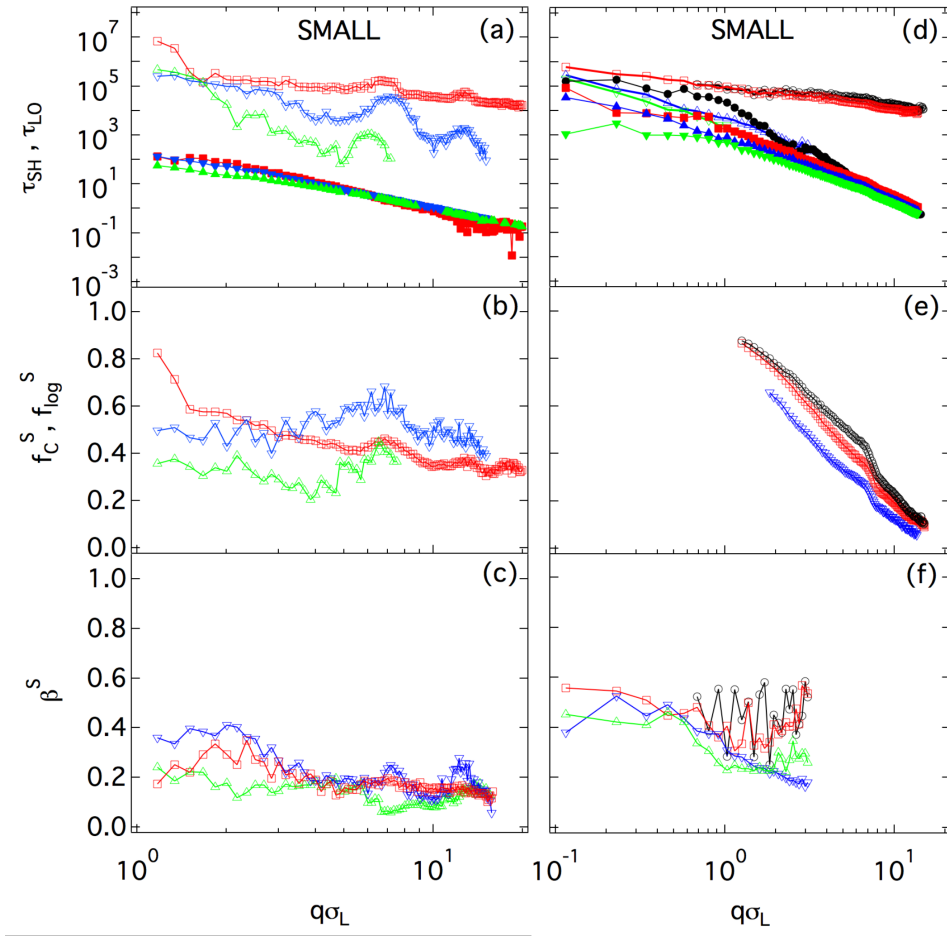


FIG. S9: Parameters obtained by fitting Eq.6 to  $f(q, \Delta t)$  from experiments for  $x_s = 0.01$ ,  $\delta = 0.18$  and  $\phi = 0.60$  ( $\triangle$ ),  $0.61$  ( $\nabla$ ),  $0.625$  ( $\square$ ) (Left) and  $\delta = 0.28$   $\phi = 0.58$  ( $\triangle$ ),  $0.59$  ( $\nabla$ ),  $0.60$  ( $\square$ )  $0.61$  ( $\circ$ ) (Right). (a), (d) Long and short relaxation times of the small particles,  $\tau_{LO}$  (open symbols) and  $\tau_{SH}$  (full symbols), respectively. (b), (e): Plateau height  $f_c^S$  (b) and  $f_{log}^S$  (e), where the last is defined in Eq.7 of the main manuscript. (c), (f) Stretching exponents obtained  $\beta^S$  obtained from the fits to the long-time relaxation of the small particles.